

## THE DEVELOPMENT OF STREAMER BREAKDOWN IN NEON IN LARGE GAPS

N. S. RUDENKO and V. I. SMETANIN

Institute of Nuclear Physics, Electronics, and Automation, Tomsk Polytechnic Institute

Submitted November 30, 1970

Zh. Eksp. Teor. Fiz. 61, 146–153 (July, 1971)

An electron-optical method has been used to study breakdown in neon occurring in the center of a discharge gap in a cosmic-ray track. The time characteristics of the processes have been determined. It is shown that in neon the electron avalanche transfers to an anode streamer before the appearance of the cathode streamer.

## INTRODUCTION

THE development of spark chamber techniques,<sup>[1]</sup> which at the present time have become one of the main experimental means of studying elementary particles, has resulted in increased interest in electric breakdown in the noble gases and their mixtures, which are used in spark chambers. Thus, Davidenko et al.<sup>[2]</sup>, on the basis of experimental studies of the electric breakdown of neon, draw the conclusion that streamer breakdown in pure neon has a number of features which are due to existence of an ionization mechanism not involving photorecombination.<sup>[3]</sup>

The present article is devoted to a study of the time characteristics of the development of the initial stages of streamer breakdown in neon, occurring in the track of a cosmic-ray particle in the center of the discharge gap. Study of the dynamics of these processes and of their dependence on specific experimental parameters presents definite interest both from the point of view of gas discharge physics and for the practical determination of optimal working parameters and possibilities of spark (streamer) chambers as charged-particle detectors.

## EXPERIMENTAL METHOD

A diagram of the experimental apparatus is shown in Fig. 1. The main elements are a high voltage generator of rectangular pulses, a spark chamber, and detection and control circuitry. In contrast to ref. 2, the recording of brief stages of the process in the chamber was accomplished by means of a pulsed image converter 6 of the type ZIM-2.<sup>[4]</sup> The high voltage generator simultaneously produced a 30 kV pulse with a 2 nsec rise time, used in the image-converter control circuit, and a pulse of controllable amplitude from 30 to 100 kV and 100 nsec duration with a variable rise time of 2–10 nsec for supplying the object of study (spark chamber) and the exposure-pulse shaping circuit from the same generator assures strict matching of the optical image to the phase of the process being studied.

Simultaneously with the recording of the optical picture of the processes in the chamber, oscillograms were taken of the exposure pulses from capacity divider 10, located directly at the anode of the image converter. The time of passage of light from the spark to the image-converter photocathode and the transit time of

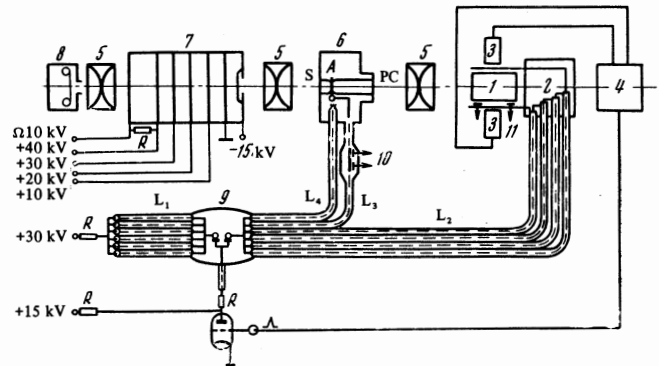


FIG. 1. Diagram of experimental equipment: 1—spark chamber, 2—cable transformer, 3—scintillation counter, 4—coincidence circuit, 5—Helios 40 objective, 6—electron-optical image converter type ZIM-2, 7—light amplifier, 8—camera, 9—three electrode spark gap, 10 and 11—capacity voltage dividers, PC—photocathode, S—screen, A—anode,  $L_1$ – $L_4$ —transmission lines.

electrons to the anode of the image converter, which decreases the exposure time, were taken into account in determining the moment of exposure. The accuracy of matching the image-converter picture to the phase of the process studied is 1.0 nsec or better. In addition, simultaneous oscillograms were made of the voltage on the chamber electrodes by means of an active divider employing type TVO resistors.

## EXPERIMENTAL RESULTS AND DISCUSSION

The apparatus described was used to measure the rate of propagation and length of the anode streamer (moving in the direction of the electron avalanche to the positive electrode of the discharge chamber) and the cathode streamer as a function of time and the electric field intensity in the chamber. The results of the measurements are shown in Fig. 2. Each ordinate value of the plots in Fig. 2 was found as the arithmetic mean of measurements of 30–40 streamers. The accuracy of the measurements was  $\pm 0.2$  mm or better. The spread in the lengths of the streamers is shown only for two curves, in order to avoid cluttering the figure. The spread increases with increasing intensity  $E_0$  and streamer length.

Characteristic photographs of successive stages in development of the discharge in a gap of length 38 mm are shown in Fig. 3. The photograph of Fig. 3a corre-

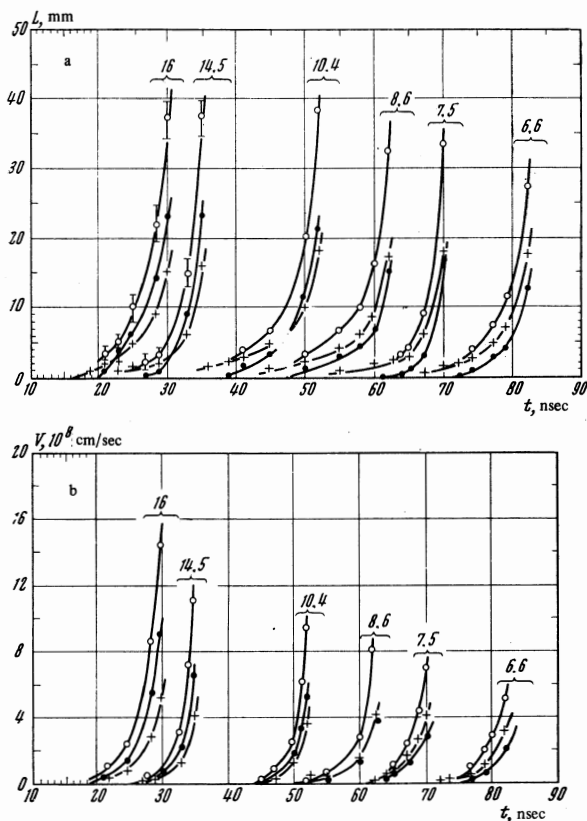


FIG. 2. Length  $L$  (a) and velocity  $V$  (b) of anode and cathode streamers as a function of time  $t$  and electric field strength in the chamber: +—anode streamer, ●—cathode streamer, ○—total streamer length. The numbers under the curves are the field strength in kV/cm.

sponds to the moment of minimal sensitivity of the experimental apparatus to light; Fig. 3g corresponds to the moment when the discharge reaches the chamber electrodes. The discharge in neon occurred in such a way that the place of origin was always distinguished; in the latter stages it had the form of a constriction. Beginning at a certain moment, at the ends of the ionized region, which is part of the electron avalanche, there appear fronts of high ionization, and extension of the radial dimensions of the ionized region is observed (Fig. 3).

With a substantial decrease in sensitivity of the image converter tube, the space between the streamers appeared in the form of a dark gap. The length of the dark gap depended on the electric field intensity in the chamber but was always less than the critical length of an avalanche in neon, calculated from the condition of equality of the fields inside and outside the shower.<sup>[5]</sup> We can assume that the electron avalanche at the moment of appearance of the streamers acquires a definite conductivity, so that distortion of the external field is obtained identically from the two ends of the conducting region. Brown<sup>[6]</sup> mentions this behavior of an avalanche. Over the entire range of intensities studied, no delay was observed in the moment of appearance of the cathode-directed streamer with respect to the moment of appearance of the accelerated ionization front moving toward the anode. The simultaneous appearance of oppositely directed streamers separated by a distance

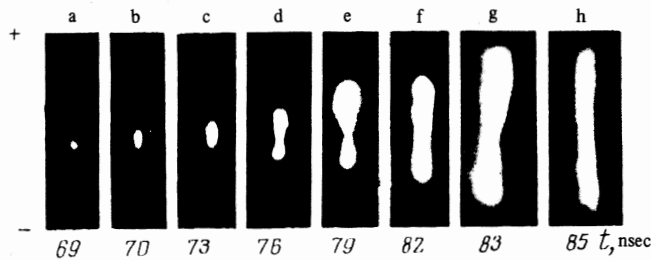


FIG. 3. Successive stages in development of a discharge in the gap,  $E_0 = 6.6$  kV/cm.

substantially greater than  $1/\alpha$  ( $\alpha$  is the first Townsend coefficient) confirms the existence of a conducting region in a "subcritical avalanche". In fact, to the extent that the electron avalanche approaches the critical number of carriers, the field of its space charge increases to a value which may be comparable with the external field  $E_0$ . At the moment when the space-charge field of the avalanche  $E_r$  approaches in value the applied field  $E_0$ , behind the avalanche in a unit time there will remain as many electrons as positive ions, and in the space behind the avalanche, as it moves toward the anode, will be left a weakly conducting channel of neutral plasma.

Simultaneous fulfillment of two conditions is necessary for appearance of a conducting region in the developing avalanche: 1)  $E_0 = E_r$ ; 2)  $1/\alpha \leq 2r_0$ . The space charge field can be determined if we assume that it is located in a sphere of radius  $r_0$ :

$$E_r = \frac{ne}{4\pi\epsilon_0 r_0^2}, \tag{1}$$

where  $n$  is the number of carriers in a sphere of radius  $r_0$ , and  $e$  is the electronic charge. Assuming that the dominant mechanism for extension of the avalanche in the initial part of its development is free diffusion, condition 1) can be written in the form  $ne/4\pi\epsilon_0 = 4.5 \bar{u}x$ , and condition 2) in the form  $E_0/4\alpha^2 = 4.5 \bar{u}x$ , where  $\bar{u}$  is the average energy of electrons in the neon.

If conditions 1) and 2) are satisfied, the number of carriers in the head of a developing avalanche for which a conducting region begins to be formed can be determined from the expression

$$n_c = \pi\epsilon_0 E_0 / e\alpha^2. \tag{2}$$

If we assume that development of an electron avalanche up to this number of carriers occurs according to the exponential law  $n = n_0 e^{\alpha vt}$ , it is possible to determine the time when the conducting region begins to form in the avalanche. In view of the absence of reliable data on electron drift velocity for large values of  $E_0/p$  ( $p$  is the gas pressure), we obtain the dependence of the electron drift velocity in neon on field strength by a simple extrapolation of the data of Healey and Reed<sup>[7]</sup> to higher values of  $E_0/p$  by means of the expression

$$V_{dr} = \sqrt{E_0/p} (1 + 10^8 / E_0^2)^{1/3}, \quad E_0 \geq 5 \text{ kV/cm} \tag{3}$$

where  $p$  is in units of torr, and  $E_0$  in V/cm.

In the portion of interest to us  $E_0 = 5-30$  kV/cm the curve  $\alpha = f(E)$  can be replaced with sufficient accuracy by a straight line given by the equation  $\alpha = (A + BE)$  with coefficient values  $A = -10^2$  cm,  $B = 16.65 \times 10^{-3} \text{ V}^{-1}$ .

	$E_0$ , kV/cm					
	16	14.5	10.4	8.6	7.5	6.6
$n_c$	$1.08 \cdot 10^6$	$1.29 \cdot 10^6$	$3.7 \cdot 10^6$	$6.5 \cdot 10^6$	$9 \cdot 10^6$	$1.4 \cdot 10^7$
$t_c$ , nsec	13.3	15.5	30.0	39.8	45.2	64.0
$\Delta t$ , nsec	4.3	5.5	6.0	7.2	7.8	13.0
$\Delta S_p$ , mm	0.5	0.75	1.15	1.67	2.04	3.94
$\Delta S_e$ , mm	$0.35 \pm 0.2$	$0.5 \pm 0.2$	$1.5 \pm 0.5$	$2.0 \pm 0.5$	$2.2 \pm 0.5$	$3.5 \pm 0.5$
$V_{ac}$ , cm/sec	$1.5 \cdot 10^7$	$1.7 \cdot 10^7$	$0.2 \cdot 10^8$	$0.2 \cdot 10^8$	$0.25 \cdot 10^8$	$0.3 \cdot 10^8$
$1/u$ , mm	0.661	0.072	0.156	0.22	0.28	0.4

Note:  $n_{cr} = 10^8$ ,  $p = 730$  torr, gas—purified neon.

The time of development of the avalanche to  $n_c$  charge carriers in its head is determined from the expression

$$t_c = \frac{10^{-6} \ln n_c}{(A + BE_0) \sqrt{E_0/p} (1 + 10^6 E_0^{-2})} \text{ (nsec).} \quad (4)$$

Calculated values of  $n_c$  and  $t_c$  are given in the table for the conditions of the experiment.

With further development of the avalanche, the increase of field strength in its front will be associated with an increase in surface charge as the result of its polarization in the external field. In this sense it is possible to speak of a critical number of particles  $n_{cr}$  in the avalanche head, at which participation of secondary processes (secondary avalanches) will determine the subsequent development of the ionization process in the directions toward the anode and cathode at the ends of the conducting region. Then the size of the conducting region along the field can be determined from the expression

$$\Delta S_p = (t_{cr} - t_c) V_{av},$$

where  $t_{cr}$  is the time at which the critical number of carriers is reached,  $t_c$  is the moment of transition of the avalanche to a conducting state, and  $V_{av}$  is the velocity of the ionization front.

The calculated values of  $\Delta S_p$ , taking into account the actual velocity of the ionization front observed experimentally, and the values of  $\Delta S_e$  obtained in experiments are given in the table. In calculation of the time  $t_{cr}$ , the value of  $n_{cr}$  was taken as  $10^8$  in the absence of better data. We have also shown in the table the values of the velocity  $V_{ac}$  at the end of the avalanche development interval, recorded experimentally. The fact that the

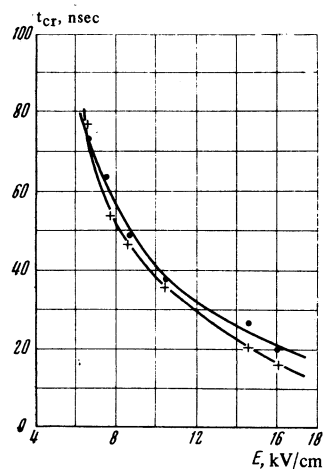


FIG. 4. Critical time in neon as a function of electric field strength: ●—experiment, +—theory.

calculated and observed values of  $t_{cr}$  and  $\Delta S$  are nearly the same can serve as the first confirmation of the ideas on which this discussion is based. The calculated values lie well within the limits determined by the experimental errors.

The dependence of the critical time on electric field intensity (for  $p = \text{const}$ ), shown in Fig. 4, was obtained on the assumption that the critical time of avalanche development corresponds to the time of appearance of the oppositely directed ionization fronts. Also shown is the function  $t_{cr} = f(E_0)$ , calculated from Eq. (4). The theoretical and experimental curves are in very good agreement for low field strengths. The maximum disagreement of the curves is 20% at a field strength  $E_0 = 16$  kV/cm. This lack of agreement of times at large fields may be explained, for example, by a slowing down of the rate of development of the ionization process as a result of the rapid increase in the radius of the avalanche head due to electrostatic repulsion. The electrostatic repulsion effect should appear more strongly at higher values of electric field.

It should be noted that in the avalanche development interval considered from  $t_c$  to  $t_{cr}$ , beginning with a number of carriers  $\sim 10^6$ , the avalanche is already transformed to an anode streamer, since the rate of propagation of the ionization front becomes higher than the initial drift velocity of the electrons, and the avalanche acquires the nature of a plasma filament. The rate of propagation of the ionization front to the anode at the end of this interval increased by 2.5–3 times in comparison with the initial electron drift velocity for a given value of electric field strength (see the table). The ratio  $V_{ac}/V_{av}(E)$  is a weak function of the initial field strength. The law of multiplication of the carriers in the anode-directed streamer at the beginning of its development does not differ substantially from the law of multiplication of the carriers in the avalanche. This idea is favored by the agreement of the theoretical and experimental values of  $t_{cr}$ , where the times  $t_{cr}$  were calculated by us from the same formula as in the initial stages of avalanche development. We note also that during the growth of the anode streamer, the intensity of its radiation does not increase substantially, while at the time  $t_{cr}$  a strong increase in the intensity is observed. Thus, in neon, as in other gases,<sup>[5,8]</sup> the avalanche is transformed at the beginning to an anode streamer. This fact was not noted by Davidenko et al.<sup>[2]</sup> The appearance of the cathode streamer and the simultaneous acceleration of the anode streamer can be explained by participation of secondary processes in the gas. The experimentally measured streamer velocities can be reduced to the following (see Fig. 2).

The anode-directed and cathode-directed streamers at the moment of their beginning have the same initial velocity,  $\sim 0.2 \times 10^8$  cm/sec. With further development of the streamers the cathode streamer velocity is less than the anode streamer velocity for an electric field strength in the chamber  $E_0 < 8.5$  kV/cm. For electric field strengths greater than 9 kV/cm, the cathode streamer velocity is always greater. This relation between the streamer velocities was preserved as the total length of the streamers was varied from 3 to 38 mm, i.e., over the whole range of lengths recorded. A similar relation of the velocities was also observed by

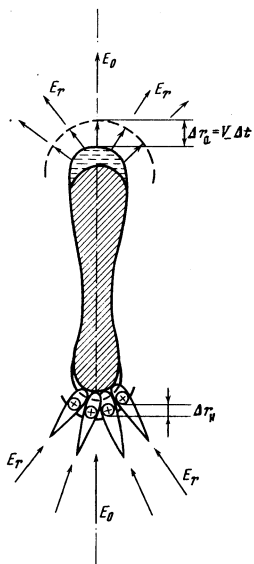


FIG. 5. Schematic representation of development of oppositely directed streamers.

Davidenko et al. in a smaller range of lengths. The difference in the velocities of propagation of the oppositely directed streamers indicates the different mechanisms of their formation. As the two oppositely directed streamers develop, the conditions in the head of each will change in accordance with the change in the radial component of the electric field, which is determined by Eq. (1) and depends on the radii of curvature of the streamer ends. The different widening of the channel in the anode and cathode branches is determined principally by the direction of the radial field: on the anode side it leads to a general diffusion of the ionization front, and on the cathode side to a concentration (see Fig. 5).

The radius of curvature of the anode branch of the streamer will be due to the drift of the electrons located there in the radial direction with a velocity  $V_- = f(E_r)$ . The radius of curvature of the cathode streamer may be due to the diffusion radius of the secondary shower developing in the field  $E_r$  during the same time, since a positive space charge will be created by the secondary avalanches mainly in the end region.

In analysis of the image-converter pictures it was found that in 70% of the cases the cathode streamer had a smaller diameter than the anode streamer. This confirms the assumptions described above regarding streamer velocities.

In Fig. 6 we have shown the streamer velocities as a function of their total length for different field strengths. The anode and cathode streamer velocities increase monotonically with increasing streamer length up to a certain value at which acceleration of the streamers occurs. The monotonic rise in streamer velocity with increasing length is in good agreement with the mathematical model proposed by Lozanskiĭ and Firsov.<sup>[9]</sup> At a certain streamer length, acceleration occurs, which is expressed in a sharp increase in the slope of the functions  $V_{\pm} = f(\Sigma l)$  shown in Fig. 6. The total length at which acceleration of the streamers begins depends on the electric field strength and decreases with increasing  $E_0$ . The existence of two stages in the development of a streamer moving to the cathode has also been observed in nitrogen by Wagner<sup>[10]</sup> and has been explained by the

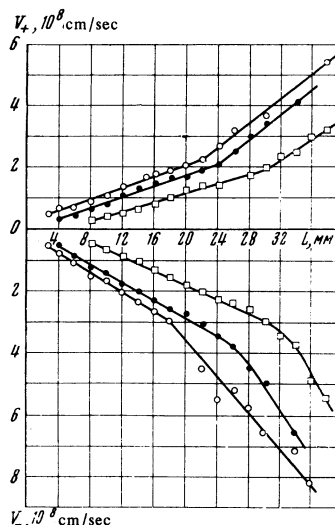


FIG. 6. Streamer velocity as a function of total length:  $\circ$ — $E_0 = 16$  kV/cm,  $\bullet$ — $E_0 = 14.5$  kV/cm,  $\square$ — $E_0 = 10.4$  kV/cm.

occurrence of photoionization at the cathode. In our case, processes at the cathode cannot affect the development of the streamer, since the dimensions of the discharge gap are considerably greater than the streamer length at which the acceleration sets in. The simultaneous acceleration of the anode and cathode streamers also indicates that the acceleration in streamer development (propagation) cannot be due to processes at the electrodes. The acceleration of the streamers can be explained by the fact that, when streamers of significant length are attained, the field strength at the ends of the streamer reaches a value at which fluctuations in the development of secondary avalanches in front of the streamer are increased. This leads to a decrease in the radius of the streamer ends and to a still greater rise in field intensity at that point. An increase in the fluctuation in streamer development with increasing  $E_0$  is indicated by the data of Fig. 2. Lozanskiĭ and Firsov<sup>[9]</sup> have suggested the possibility that the stability of the streamers is destroyed.

It should be mentioned that oscillographic studies have shown that the moment of the sharp drop in the field strength applied to the gap coincides with the moment of appearance of the oppositely directed ionization fronts, i.e., of the streamers (the moment  $t = 76$  nsec, Fig. 3). At this moment the processes in the discharge gap are obviously accompanied by a large current in the external circuit. We note also that the drop in field strength in the discharge gap occurs in two stages. The first or steep stage goes into a flat portion whose width depends on the electric field strength, and for low field strengths no boundary is observed between the two stages. An interesting fact obtained from simultaneous analysis of optical images of the discharge and oscillograms of the pulses in the chamber is the coinciding of the moment of time corresponding to the beginning of the flat portion with the moment of beginning of the second stage of streamer acceleration. The decrease in slope of the falling field-strength curve with a simultaneous increase in the velocity of advance of the ionization fronts in the streamer indicates a decrease in the num-

ber of electrons participating in creation of these fronts in comparison with the preceding stage. The beginning of the region of subsequent drop in field strength coincides with the moment at which the streamers touch the gap electrodes. For field strengths  $< 10$  kV/cm the uniform drop in field strength is consistent with the absence of the second stage of streamer acceleration up to the time when the streamers completely occupy the discharge gap.

The existence of similar steps in oscillograms of pulses in breakdown of medium gaps has been observed by Allen and Phillips<sup>[11]</sup> and has been associated with transitions from the avalanche (Townsend) type of breakdown to streamer breakdown. However, in our case these steps can be explained only by processes in the developing streamer without a change in the type of discharge.

<sup>1</sup>M. I. Daion, B. A. Dolgoshein, V. I. Efremenko, G. A. Laksin, and V. A. Lyubimov, *Iskrovaya kamera* (The Spark Chamber), Atomizdat, 1967.

<sup>2</sup>V. A. Davidenko, B. A. Dolgoshein, and S. V. Somov, *Zh. Eksp. Teor. Fiz.* **55**, 435 (1968) [*Sov. Phys.-JETP* **28**, 227 (1969)].

<sup>3</sup>E. D. Lozanskiĭ, *Zh. Tekh. Fiz.* **38**, 1563 (1968) [*Sov. Phys.-Tekh. Phys.* **13**, 1269 (1969)].

<sup>4</sup>Yu. E. Nesterikhin and R. I. Soloukhin, *Metody skorostnykh izmereniĭ v gazodinamike i fizike plazmy* (Methods of Velocity Measurement in Gas Dynamics and Plasma Physics), Nauka, 1967.

<sup>5</sup>H. Raether, *Electron Avalanches and Breakdown in Gases*, Butterworths, London, 1964. Russian translation, Mir, 1968.

<sup>6</sup>S. C. Brown, *Basic Data of Plasma Physics*, New York, Wiley, 1959. Russian transl., *Elementarnye protsessy v plazme gazogo razryada*, Gosatomizdat, 1961.

<sup>7</sup>R. H. Healey and I. W. Reed, *The Behavior of Slow Electrons in Gases*, Sydney, 1941.

<sup>8</sup>H. Tholl, *Z. Naturforsch.* **19a**, 346 (1964).

<sup>9</sup>É. D. Lozanskiĭ and O. B. Firsov, *Zh. Eksp. Teor. Phys.* **56**, 670 (1969) [*Sov. Phys.-JETP* **29**, 367 (1969)].

<sup>10</sup>K. H. Wagner, *Z. Physik* **189**, 465 (1966).

<sup>11</sup>K. R. Allen and K. Phillips, *Proc. Roy. Soc. (London)* **278A**, 188 (1964).

Translated by C. S. Robinson